



Aalborg Universitet

AALBORG UNIVERSITY  
DENMARK

## A New Lumped-Charge Modeling Method for Power Semiconductor Devices

Duan, Yaoqiang; Iannuzzo, Francesco; Blaabjerg, Frede

*Published in:*

I E E E Transactions on Power Electronics

*DOI (link to publication from Publisher):*

[10.1109/TPEL.2019.2938104](https://doi.org/10.1109/TPEL.2019.2938104)

*Publication date:*

2020

*Document Version*

Accepted author manuscript, peer reviewed version

[Link to publication from Aalborg University](#)

*Citation for published version (APA):*

Duan, Y., Iannuzzo, F., & Blaabjerg, F. (2020). A New Lumped-Charge Modeling Method for Power Semiconductor Devices. *I E E E Transactions on Power Electronics*, 35(4), 3989 - 3996. [8818346]. <https://doi.org/10.1109/TPEL.2019.2938104>

### General rights

Copyright and moral rights for the publications made accessible in the public portal are retained by the authors and/or other copyright owners and it is a condition of accessing publications that users recognise and abide by the legal requirements associated with these rights.

- Users may download and print one copy of any publication from the public portal for the purpose of private study or research.
- You may not further distribute the material or use it for any profit-making activity or commercial gain
- You may freely distribute the URL identifying the publication in the public portal -

### Take down policy

If you believe that this document breaches copyright please contact us at [vbn@aub.aau.dk](mailto:vbn@aub.aau.dk) providing details, and we will remove access to the work immediately and investigate your claim.

# A New Lumped-Charge Modeling Method for Power Semiconductor Devices

Yaoqiang Duan, *Student Member, IEEE*, Francesco Iannuzzo, *Senior Member, IEEE*, and Frede Blaabjerg, *Fellow, IEEE*

**Abstract-** This paper proposes a new lumped-charge model for power semiconductor devices. The existing lumped-charge model, due to its linear modeling method, has some limitations that will impair the accuracy of the model. Firstly, this paper analyses the restriction of traditional lumped-charge modeling method. Then, based on the limitation analysis, a new lumped-charge modeling method is presented and improves the accuracy of the traditional one while keeping its advantages. In this new model, the relationship between the ambipolar current and the lumped charges in the power devices is redefined. Finally, the new method is implemented to an Insulated Gate Bipolar Transistor (IGBT) model and PiN freewheeling diode. The accuracy of the models is verified by experiment including both the static and transient characteristics and compared with the traditional IGBT model.<sup>1</sup>

## I. INTRODUCTION

Power devices modelling provides a very efficient and low-cost way to study the characteristics of them for improving the reliability and efficiency of converters. With the promotion of design standards, circuit designers of power electronic systems are calling for better power device models. To reduce system redundancy and costs, the model should get more accurate simulation results. For analysis of the abnormal operation and failure mechanism, the model should also be physics-based. Among the many physics-based models [1-7], the lumped-charge model is one of the promising models.

The concept of the lumped-charge model for power semiconductor devices was first introduced by C. L. Ma *et al.* in 1991 [8]. Based upon the lumped parameter approach initially developed by J. G. Linvill's [9], some charge storage nodes are put in different parts of the devices to present the charge control effects. The lumped-charge approach is a physics-based power semiconductor model which means that it could not only model the electrical characteristics of device terminals but also provide additional insight into the transportation process of the internal carriers.

Compared with other power semiconductor physical models, the lumped-charge approach doesn't need to solve the second order partial differential equation—the ambipolar diffusion

equation (ADE) in the drift region which is derived from the current transport equation and the carrier continuity equation [8, 10]. In the lumped-charge model, these two kinds of equations are expressed by the integration of them in a discrete spatial form and rewritten according to hole and electron respectively. This feature allows us to separately consider the roles of hole's and electron's currents in the devices, and avoid the high-level injection approximations. Then some lumped charges could be put into the drift region to present the charge control effects described by these two physical equations [7]. Through this method, the lumped-charge approach avoids the complex differential equation solution and make a good compromise between computation time and accuracy. Furthermore, it is more suitable for being implemented into circuit simulation platforms, such as PSPICE and SABER. On the other hand, the quantity and difficulty of the parameter extraction are much less compared to the other physical models [7]. Therefore, the lumped-charge model is more suitable for general circuit designers and researchers.

Due to the above advantages, the lumped-charge model, after being proposed, has been quickly applied to various power semiconductor devices, such as power diode [11], MOSFET [12], GTO [13, 14] and IGBT [7]. However, one can assume that what is gained in simplicity is lost in calculation accuracy. Both the simplicity and relatively poor accuracy come from the finite-difference method. Employing the curve-fitting method, the lumped-charge model could also get a good simulation result under a single operating condition, while the results would be inaccurate in other operating conditions with the same parameters, which substantially limits the use of it. In [15] M. Bellini *et al.* propose an improved lumped-charge model for high voltage power diode. This paper extends the model including impact ionization, while the modelling method is consistent with the traditional approach.

The target of this paper is to present a new lumped-charge modeling method with higher accuracy for power semiconductor devices while maintaining the advantages of this kind of model. Firstly, this paper analyses the limitation of the traditional lumped-charge model. Then an improved method is proposed to counteract the impact of these restrictions. Finally, the proposed modeling method is implemented to an IGBT and PiN diode model and verified by experiment including both the static and transient characteristics.

---

This work was supported by the National Natural Science Foundation of China under Grant 51490681, by National Key Basic Research Program of China 973 Program under Grant 2015CB251004.

Y. Duan is with School of Electrical and Electronics Engineering, Huazhong University of Science and Technology, Wuhan 430074, China (E-mail: duanyaoqiang@hust.edu.cn).

F. Iannuzzo and F. Blaabjerg are with the Energy Technology Department, Aalborg University, Aalborg East 9220, Denmark (E-mail: fia@et.aau.dk).

## II. THE IMPROVEMENT OF LUMPED-CHARGE MODEL

The role of lumped charge modeling method in the physical model of IGBT is to characterize the movement and distribution of carrier in the base region. The lumped charge model calculates the distribution of carriers as the solution of the model in an equivalent way without presupposing the specific distribution function of carriers [7]. The relatively low simulation results of the traditional lumped-charge model have been pointed out in [16], while there is no specific analysis about it. In this section, the limitation of the traditional approach is analyzed, and then an improved method is presented to reduce the impact of these limitations.

### A. The Limitation Analysis of Traditional Lumped-charge Model

As recommended in [11], three lumped-charge nodes are used to reproduce the carrier distribution in the base region (Fig. 1).

As shown in Fig. 1,  $p_2$ ,  $p_3$ , and  $p_4$  represent the hole concentration at each lumped-charge node in the base region, and the drift region width  $d$  is divided into two regions with width  $d_{23}$  and  $d_{34}$  respectively. The width of the two sub-regions in this model is equal.  $I_C$  is the total current flowing through the base region and equals the sum of the hole current and the electron current.  $x_2$ ,  $x_3$ , and  $x_4$  represent the coordinate position of  $p_2$ ,  $p_3$ , and  $p_4$ .

In the typical and traditional lumped-charge model proposed in [11], firstly, the assumption of linear distribution between  $p_2$ ,  $p_3$ , and  $p_4$  is adopted. So, the hole current  $i_{p23}$  and electron current  $i_{n23}$  flowing from  $p_2$  to  $p_3$  are defined as

$$\begin{cases} i_{p23} = qA \frac{p_2 + p_3}{2} \mu_p E - qAD_p \frac{p_2 - p_3}{d_{23}} \\ i_{n23} = qA \left( \frac{p_2 + p_3}{2} + N_B \right) \mu_n E + qAD_n \frac{p_2 - p_3}{d_{23}} \end{cases} \quad (1)$$

where  $q$  is electron charge,  $A$  is the device active area,  $N_B$  is the doping concentration of the drift region, and  $\mu_p$  and  $\mu_n$  are the hole mobility and electron mobility. As specified in Fig. 1,  $d$  is the drift region width,  $E$  is electric field intensity.

Based on the approximations below,

$$E = \frac{v_{23}}{d_{23}}, \quad (2)$$

$$\frac{p_2 + p_3}{2} \approx p_3, \quad (3)$$

equation (1) could be expressed as:

$$\begin{cases} i_{p23} = \frac{q_{p3}}{T_{p23}} \frac{v_{23}}{V_T} + \frac{q_{p2} - q_{p3}}{T_{p23}} \\ i_{n23} = \frac{q_{p3} + Q_M}{T_{n23}} \frac{v_{23}}{V_T} - \frac{q_{p2} - q_{p3}}{T_{n23}} \end{cases}, \quad (4)$$

where  $q_{p2} = qAdp_2$ ,  $q_{p3} = qAdp_3$ .  $v_{23}$  is the voltage drop from node  $p_2$  to  $p_3$ ,  $T_{p23}$  and  $T_{n23}$  are the hole transit time and electron transit time between the adjacent nodes  $p_2$  and  $p_3$ .  $V_T$  is the thermal voltage. The first term of the right side of (4) represents the drift current and the second term is the diffusion current.

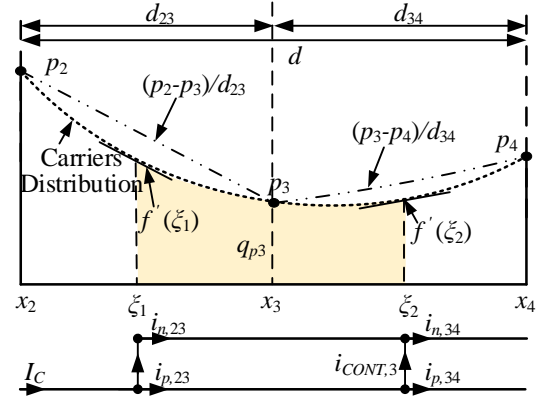


Fig. 1 The traditional lumped-charge modeling method of the drift region.

The similar hole current expression between  $p_3$  and  $p_4$  is

$$\begin{cases} i_{p34} = \frac{q_{p3}}{T_{p34}} \frac{v_{34}}{V_T} + \frac{q_{p3} - q_{p4}}{T_{p34}} \\ i_{n34} = \frac{q_{p3} + Q_M}{T_{n34}} \frac{v_{34}}{V_T} - \frac{q_{p3} - q_{p4}}{T_{n34}} \end{cases}, \quad (5)$$

where  $q_{p4} = qAdp_4$ .  $v_{34}$  is the voltage drop from node  $p_3$  to  $p_4$ ,  $T_{p34}$  and  $T_{n34}$  are the hole transit time and electron transit time between the adjacent nodes  $p_3$  and  $p_4$ .

Another important equation in the lumped-charge model, which is derived from the carrier continuity equation, is the charge-control equation. The hole continuity equation is given by

$$-\frac{dJ_p}{qdx} = \frac{d\delta p}{dt} + \frac{\delta p}{\tau_p}, \quad (6)$$

where  $J_p$  is the hole current density,  $\delta p$  is the concentration of excess hole carriers, and  $\tau_p$  is the carrier lifetime of hole carriers.

The equation (6) is multiplied by the unit charge  $q$  and the effective conductive area  $A$  of the chip, and integrated along the positive direction of the current from  $x_2$  to  $x_4$  in Fig. 1 could get:

$$\begin{aligned} i_{p23} - i_{p34} &= -A \times \int_{x_2}^{x_4} dJ_p \\ &= qA \times \frac{d(\int_{x_2}^{x_4} \delta p dx)}{dt} + qA \times \frac{\int_{x_2}^{x_4} \delta p dx}{\tau_p} \end{aligned} \quad (7)$$

where  $dJ_p$  is the differential term of hole current density,  $dx$  is the differential term of space distribution position  $x$ .

In [5], the authors use another assumption:

$$q_{p3} \approx qA \cdot (\int_{x_2}^{x_4} \delta p dx), \quad (8)$$

where  $Q_{Bp} = qAdp_0$ , and  $p_0$  is the hole concentration of the drift region in thermal equilibrium. Thus, equation (7) could be expressed as:

$$i_{p23} - i_{p34} = \frac{q_{p3} - Q_{Bp}}{\tau_p} + \frac{dq_{p3}}{dt}, \quad (9)$$

which means the concentration of excess hole carriers in the drift region integrated along the direction from  $x_2$  to  $x_4$  is equal to  $q_{p3}$ , cause  $Q_{Bp}$  is very small compared to  $q_{p3}$  when there are obvious current flows through IGBT. Actually, as shown in (4),  $q_{p3}=qAdp_3$ . Logically speaking, this assumption will bring errors to the traditional lumped-charge model.

Assuming the distribution function of carriers in the base region is  $f(x)$ . Since the carrier distribution is continuous, according to the Lagrange's Mean Value Theorem, we could consider that there are two points  $\xi_1$  and  $\xi_2$  among the adjacent nodes to meet the equations (Fig. 1):

$$\begin{cases} f'(\xi_1) = \frac{p_2 - p_3}{d_{23}} \\ f'(\xi_2) = \frac{p_3 - p_4}{d_{34}} \end{cases} \quad (10)$$

From the point of view of model calculation, if the distribution of excess carriers follows the dashed curve in Fig. 1, the charge  $q_{p3}$  obtained from (9) in traditional lumped-charge modeling method equals the charge of carriers between  $\xi_1$  and  $\xi_2$ , approximately.

As discussed above, the current  $i_{p23}$  is the hole current flowing into the drift region and the current  $i_{p34}$  is the hole current flowing out of it. Assuming the current  $i_{p23}$  is fixed, the value of  $i_{p34}$  will change with the charge  $q_{p3}$  according to (9). However, the value of  $i_{p34}$  is actually governed by the total charge  $Q$  ( $Q$  equals the integration of excess hole carriers concentration from  $x_2$  to  $x_4$  multiplied by the unit charge  $q$  and the effective conductive area  $A$ ) in the base region in a real power device. Based on the analysis above, there is a big difference between the charge  $Q$  and charge  $q_{p3}$  (see Fig. 1). This difference is the main reason for the inaccuracy of the traditional lumped-charge model.

The effects of this inaccuracy on the electrical characteristics of power devices mainly manifest in the following two aspects:

(1) For the static characteristics, the conductivity modulation effect (CME) in power semiconductor devices, especially for bipolar devices is very remarkable on the regulation of the forward voltage drop [17]. The CME is proportional to the concentration of excess carriers. The incorrect calculation of the charge  $Q$  will have a negative influence on the simulation of the forward voltage drop in static operations.

(2) For the dynamic characteristics, the reverse recovery current or tail current of power semiconductor devices is closely related to the carrier distribution in the drift region [17]. The incorrect calculation of the charge  $Q$  will result in a bad description of the reverse recovery current or tail current. Furthermore, this inaccuracy will also cause a poor simulation for the power losses and shoot voltage or current in power electronic systems.

By using parameters adjustment, the traditional lumped-charge model could also give a better fit to the experiment results, but the model will lose its physics-based status and be only effective in some fixed conditions [16].

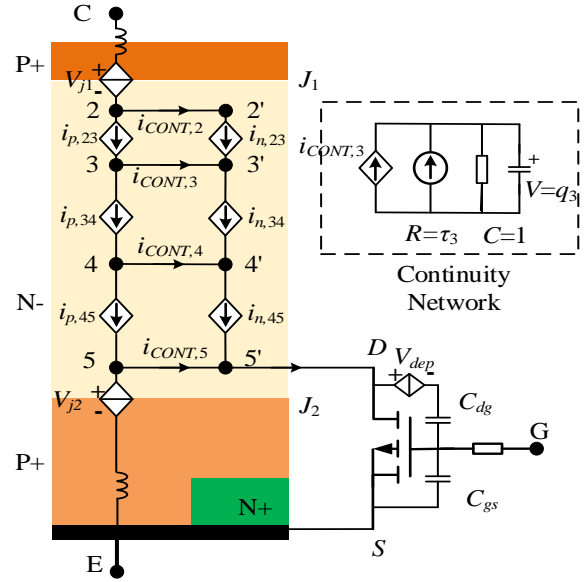


Fig. 2 The IGBT lumped-charge model proposed in [18].

To improve the accuracy of the traditional lumped-charge model, Aalborg University propose the IGBT lumped charge model which uses four lumped charge nodes to describe the movement and distribution of carriers in the drift region [18]. In addition, in order to further improve the simulation accuracy of the model, the average partition of the drift region in Fig. 1 is changed to non-average partition. The specific process will be discussed in conjunction with the model equation. The schematic diagram of the model modeling method is shown in Fig. 2.

In Fig. 2, there are four lumped charge nodes putted in the drift region. The improved lumped-charge modelling method is shown in Fig. 3.  $p_2$  at the left edge of the drift region,  $p_3$  and  $p_4$  at the middle of the drift region, and  $p_5$  at the right edge of the drift region. The drift with width  $d$  is divided into three regions with width of  $\gamma_1 d$ ,  $\gamma_2 d$  and  $\gamma_3 d$ , respectively.  $\gamma_1$ ,  $\gamma_2$  and  $\gamma_3$  are zoning coefficients, which satisfy the following relations:

$$\gamma_1 + \gamma_2 + \gamma_3 = 1. \quad (11)$$

In Fig. 3, according to the traditional lumped-charge modeling method, the hole current  $i_{p23}$  and electron current  $i_{n23}$  flowing from  $p_2$  to  $p_3$  are defined as:

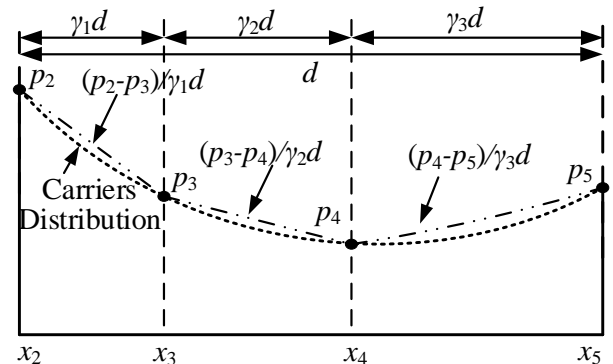


Fig. 3. The improved lumped-charge modelling method in [18].

$$\begin{cases} i_{p23} = \frac{\gamma_1 \cdot q_{p3}}{T_{p23}} \frac{v_{23}}{V_T} + \gamma_1 \cdot \frac{q_{p2} - q_{p3}}{T_{p23}} \\ i_{n23} = \frac{\gamma_1 \cdot (q_{p3} + Q_M)}{T_{n23}} \frac{v_{23}}{V_T} - \gamma_1 \cdot \frac{q_{p2} - q_{p3}}{T_{n23}} \end{cases} \quad (12)$$

The charge control equation could be expressed as:

$$i_{p23} - i_{p34} = \frac{d(\gamma_1 + \gamma_2) \cdot q_{p3}}{dt} + (\gamma_1 + \gamma_2) \cdot \frac{q_{p3} - Q_M}{\tau_p} \quad (13)$$

The hole current  $i_{p34}$ ,  $i_{p45}$ , and electron current  $i_{n34}$ ,  $i_{n45}$ , flowing from  $p_3$  to  $p_4$ , and  $p_4$  to  $p_5$  could be defined in a similar way.

Though the improved IGBT model in Fig. 2 could have better simulation accuracy, it still uses the traditional lumped-charge modeling method. So, the limitations of the traditional model we discussed above are also the IGBT model in Fig. 2. And the model will be used to compare with the new lumped-charge modeling method proposed in this paper later.

### B. The Improved Lumped-charge Model

According to the analysis in the previous section, from the view of carrier distribution, the traditional lumped charge modeling method firstly defines the carrier concentration at the points in the drift region, and then uses the assumption that the carriers are linearly distributed between adjacent charge points, and then solves the current equations and the charge control equations. The definition of lumped-charge in traditional model is actually the product of the excess carrier concentration at the corresponding charge point and the volume of the drift region. Based on the previous analysis, this definition has no practical physical significance.

Consider the charge control equation, the important physical quantity affecting the electrical characteristics of power semiconductor devices is the excess charge of carriers in the drift region, rather than the specific distribution. Therefore, this paper will change the way of solving the model, redefine the physical meaning of the lumped-charges, and derive the current equation and charge control equation under the new lumped-charge modeling method. The schematic diagram of the modeling method is shown in Fig. 4. The traditional modeling method first defines the concentration of lumped-charge points and then obtains the quantity of them. In the new modeling method, the lumped-charge quantity will be defined firstly, and then the concentration of lumped charge points will be obtained.

In Fig. 4, corresponding to Fig. 3, the drift region is also divided into three regions, each with a width of  $d/3$ . The actual charge quantities in each region are defined as lumped-charges. They are  $Q_3$ ,  $Q_4$ , and  $Q_5$ , respectively.  $p_2$ ,  $p_3$ ,  $p_4$ , and  $p_5$  represent the hole concentration at boundaries of these regions.

In Fig. 4, the hole current  $i_{p34}$  and electron current  $i_{n34}$  flowing from  $Q_3$  to  $Q_4$  are defined as:

$$\begin{cases} i_{p34} = qAu_p p_3 E + \frac{Q_3 - Q_4}{T_{p34}} \\ i_{n34} = qAu_n (p_3 + N_B) E - \frac{Q_3 - Q_4}{T_{n34}} \end{cases} \quad (14)$$

where  $\mu_p$  is the hole mobility,  $\mu_n$  is the electron mobility and  $E$  is the electric field.  $T_{p34}$  and  $T_{n34}$  are the hole transit time and electron transit time between the nodes  $Q_3$  and  $Q_4$ .

So, here we meet the problem, How to define the meaning of  $T_{p34}$  and  $T_{n34}$  between the nodes  $Q_3$  and  $Q_4$ ?

Hole diffusion current  $i_{diffp}$  and electron diffusion current  $i_{diffn}$  are defined as [19]:

$$\begin{cases} i_{diffp} = -qAu_p V_T \frac{dp(x)}{dx} \\ i_{diffn} = qAu_n V_T \frac{dp(x)}{dx} \end{cases} \quad (15)$$

The current equation can be expressed in the following differential form:

$$\begin{cases} i_{diffp} = qAu_p V_T \frac{p(x)dx - p(x+dx)dx}{(dx)^2} \\ i_{diffn} = -qAu_n V_T \frac{n(x) - n(x+dx)}{(dx)^2} \end{cases} \quad (16)$$

where,  $p(x)$  and  $n(x)$  are the spatial distribution functions of holes and electrons in the drift region, respectively.

According to (16), by extending the differential term  $dx$  of spatial distribution, the hole and electron diffusion current between two regions with the same volume can be approximately defined as:

$$\begin{cases} i_{diffp} = qAu_p V_T \frac{\int_{x-\Delta x}^x p(x)dx - \int_x^{x+\Delta x} p(x)dx}{(\Delta x)^2} \\ i_{diffn} = -qAu_n V_T \frac{\int_{x-\Delta x}^x n(x)dx - \int_x^{x+\Delta x} n(x)dx}{(\Delta x)^2} \end{cases} \quad (17)$$

As shown in Fig. 4, the region where  $Q_3$  and  $Q_4$  are located has the same volume, so that  $x_2$  is taken as the initial position of the integral term. Therefore, the hole diffusion current  $i_{diffp34}$  and electron diffusion current  $i_{diffn34}$  between lumped charges  $Q_3$  and  $Q_4$  in Fig. 4 can be expressed as:

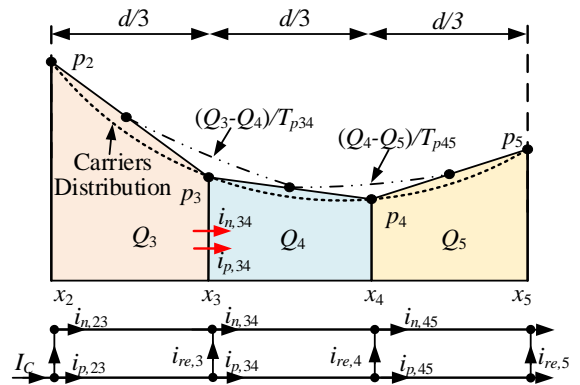


Fig. 4 The improved lumped-charge modelling method.

$$\begin{cases} i_{diffp34} = qA u_p V_T \frac{\int_{x_2}^{x_3} p(x)dx - \int_{x_3}^{x_4} p(x)dx}{(d/3)^2} = u_p V_T \frac{Q_3 - Q_4}{(d/3)^2} \\ i_{diffn34} = -qA u_n V_T \frac{\int_{x_2}^{x_3} p(x)dx - \int_{x_3}^{x_4} p(x)dx}{(d/3)^2} = -u_n V_T \frac{Q_3 - Q_4}{(d/3)^2} \end{cases} \quad (18)$$

Thus, the equation of hole current and electron current for  $Q_3$  and  $Q_4$  between adjacent lumped-charges expressed by (14) can be further expressed as follows:

$$\begin{cases} i_{p34} = \frac{q_{p3}}{T_{p34}} \frac{v_{34}}{V_T} + \frac{Q_3 - Q_4}{T_{p34}} \\ i_{n34} = \frac{q_{p3} + Q_M}{T_{n34}} \frac{v_{34}}{V_T} - \frac{Q_3 - Q_4}{T_{n34}} \end{cases} \quad (19)$$

where,  $q_{p3} = qAp_3d/3$ ,  $Q_M = qAN_Bd/3$ . The hole transit time  $T_{p34}$  and the electron transit time  $T_{n34}$  are defined as:

$$\begin{cases} T_{p23} = \frac{(d/3)^2}{u_p V_T} \\ T_{n23} = \frac{(d/3)^2}{u_n V_T} \end{cases} \quad (20)$$

Similarly, current equations of other lumped-charge nodes can be established. Besides, there is still a problem in the current equation (19) that how to determine the relationship between charge quantities  $q_{p2}$ ,  $q_{p3}$ ,  $q_{p4}$ ,  $q_{p5}$  and  $Q_3$ ,  $Q_4$ ,  $Q_5$ . In this paper, the trapezoidal area between boundary concentration is used to approximate the two-dimensional distribution area of equivalent lumped-charge, and can be expressed as follows:

$$\begin{cases} Q_3 = \frac{q_{p2} + q_{p3}}{2} \\ Q_4 = \frac{q_{p3} + q_{p4}}{2} \\ Q_5 = \frac{q_{p4} + q_{p5}}{2} \end{cases} \quad (21)$$

For the lumped-charge model, another important equation is charge control equation, according to Fig. 4, it can be written as:

$$i_{p23} - i_{p34} = \frac{dQ_3}{dt} + \frac{Q_3 - Q_m}{\tau_p} \quad (22)$$

In the new lumped charge modeling method, the minority carrier charge  $Q_m$  in the drift region under thermal equilibrium can be expressed as follows:

$$Q_m = qA \frac{d}{3} \frac{n_i^2}{N_B} \quad (23)$$

Please note that in (19) and (22), the meaning of  $q_{p3}$  is different from  $Q_3$  compared with equation (4) and (9). In the traditional lumped-charge model, the distribution of carriers in the drift region is linear. However, in the proposed approach, the relationship between the lumped charges and the boundary concentration of charges is linear whereas the distribution of carriers is nonlinear. In the new lumped-charge model, the

error between the theoretical charge and the actual charge in the drift region can be seen as the error between the trapezoidal area represented by  $Q_3$ ,  $Q_4$  and  $Q_5$  in Fig. 4 and the area surrounded by the carriers distribution represented by dotted lines. Compared with the traditional lumped charge modeling method, the error has been significantly improved.

According to [20], the electron current at the edge of PN junction is governed by the equation  $i_{n,23} = \lambda(q_{p2})^2$ , where  $\lambda$  is injection coefficient of electrons and  $q_{p2} = qAdp_2$ . Thus, the hole current flowing through the PN junction could be given by

$$i_{p,23} = 2 \cdot \frac{q_{p2}}{T_{p23}} \frac{v_{23}}{V_T} - \lambda \cdot \frac{\mu_p}{\mu_n} q_{p2}^2 \quad (24)$$

where the hole transit time  $T_{p23} = d^2/(3V_T\mu_p)$ .

Here, all the equations of the proposed new lumped-charge model for drift region of power semiconductor devices are deduced.

### III. APPLICATION OF THE NEW LUMPED-CHARGE MODEL

#### A. Model Implementation

The proposed approach has been verified by an IGBT and PiN diode model. In this paper, only the modeling method of the drift region is introduced. For the lumped-charge method is used to model the drift region, the proposed approach is applied in and used to improve the IGBT drift region model established in [18]. An IGBT physical model comprises four parts: the drift region model, the collector PN junction model, the emitter PN junction model, and the MOS part model. Except for the drift region, the other parts of the IGBT model could be found in [7]. In this paper, we use the IGBT model in [18] as the traditional lumped-charge (LC) model.

For the simulation of the turn-on behavior of IGBT, a physical PiN diode model is also needed to do the co-simulation. In this paper, we use the PiN diode model in [11] as the traditional LC model. A PiN diode physical model comprises three parts: the drift region model, the anode PN junction model, and the cathode N-N<sup>+</sup> junction model. Except for the drift region, the other parts of the model could be found in [11]. The equivalent circuit of the new LC diode model is shown in Fig. 5. Like the IGBT model, the drift region of the diode is modeled by the proposed LC approach. Both the traditional and new LC model has been conceived in the form of an equivalent circuit and implemented into the PSPICE simulator. The specific process of model implementation can be referred to in [7].

#### B. Experimental measurements

Then, the accuracy of the new LC model is proved by experiments of Infineon FF1000R17IE4 IGBT. Experimental data have been obtained by means of a Keysight B1506A device analyzer for the static characterization, and a triple pulse test setup with inductive load and a custom regulated thermal heater to adjust IGBT operating temperatures for the dynamic characterization (see Fig. 6) [21]. The gate voltage  $V_{GE}=15V$ , gate resistance  $R_g=1.2\Omega$ . We used a 1 GHz, 2.5 GS/s, 12-bit Teledyne-LeCroy scope HDO 6104-MS with a 400MHz voltage probe and a 30MHz (40 ns typical rise time), 6 kA Rogowski-coil CWT-30 ultra-mini current probe.



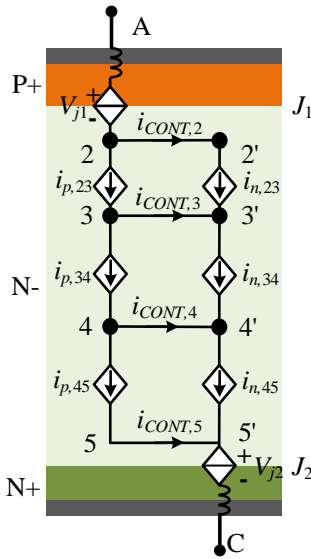


Fig. 5 The PiN diode lumped-charge model

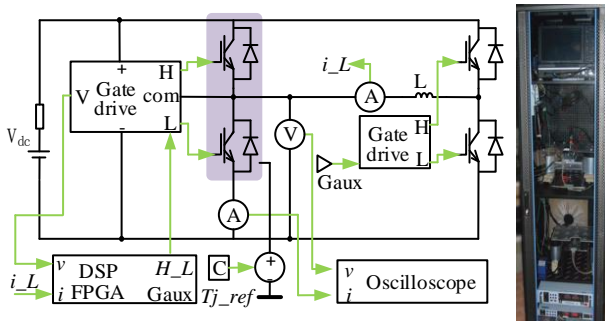


Fig. 6 The triple-pulse tester with inductive load and a custom regulated thermal heater [21].

Voltage probe offset and current probe delay has been preliminarily acquired on a calibrated load, and then the waveforms have been compensated with Matlab post-process to be able to accurately estimate the switching losses within a few percent.

### C. Model Parameters and Their Extraction

Physics-based model of IGBT gives a better insight into the complex failure mechanisms as well as a better prediction of IGBT static and transient characteristics in different operating conditions. However, the use of it accompanied by some challenges which one of them is the model parameters extraction [22].

In this paper, the parameters extraction of the lumped-charge model is divided into two steps. The first step is the parameter evaluation, including semiconductor physical parameters, device structural parameters, and parasitic circuit parameters. These parameters are not easily accessible without reverse engineering facilities or the data provided by the device manufacturers. However, in the development of physical models, with the improvement of experimental equipment, some literature has proposed a series of model parameters extraction methods [1]. These methods could be used to estimate the parameters preliminarily.

Then, the second step is using the software MBPI(Model-Based Parameter Identifier) presented in [22] to do the

optimization of parameters extracted in the first step, which can further improve the accuracy of the physical lumped-charge model. The main model parameters used in the new lumped-charge IGBT model and the traditional one is shown in TABLE I.

### D. Model Validation

#### 1) Static characteristics

As shown in Fig. 7, the proposed method obtains more accurate simulation results than the traditional LC model especially for the current between 0 to 800A at 150°C. In this stage, the carrier concentration in the drift region changed in magnitude, so the V-I characteristics exhibit non-linearity due to the different conductivity modulation. Compared with the traditional LC model, the new model could describe the conductivity modulation effect at different temperatures with higher simulation accuracy.

#### 2) Transient characteristics

The dynamic characteristics during turn-off transient have been verified as shown in Fig. 8, and turn-on is shown in Fig. 9. Compared with the traditional model, the proposed model is more in agreement with experiment especially for the vital parameters such as tail current, peak voltage, fall time,  $di/dt$  and the recovery current. Besides, in order to verify multi-working conditions, tests have been performed at several different temperatures, whose results about power losses are reported in TABLE II and TABLE III. Both the two models

TABLE I  
COMPARISON OF MODEL PARAMETERS

Model parameters	Traditional LC model	The new LC model
Device active area $A$	9 [cm <sup>2</sup> ]	9.1 [cm <sup>2</sup> ]
Width of the base region $W_B$	168 [μm]	180 [μm]
Doping of the base region $N_B$	$9.91 \times 10^{13}$ [cm <sup>-3</sup> ]	$1.5 \times 10^{14}$ [cm <sup>-3</sup> ]
Hole mobility $\mu_p$	495 [cm <sup>2</sup> /Vs]	495 [cm <sup>2</sup> /Vs]
Electron mobility $\mu_n$	1360 [cm <sup>2</sup> /Vs]	1360 [cm <sup>2</sup> /Vs]
Excess carrier lifetime $\tau_p$	0.5 [μs]	4.5 [μs]
MOS transconductance $K_p$	130 [A/V <sup>2</sup> ]	120 [A/V <sup>2</sup> ]
MOS threshold voltage $V_{th}$	5.2 [A/V <sup>2</sup> ]	6.2 [A/V <sup>2</sup> ]
Circuit stray inductance $L_s$	30 [nH]	30 [nH]
Gate resistance $R_g$	1.2 [Ω]	1.2 [Ω]

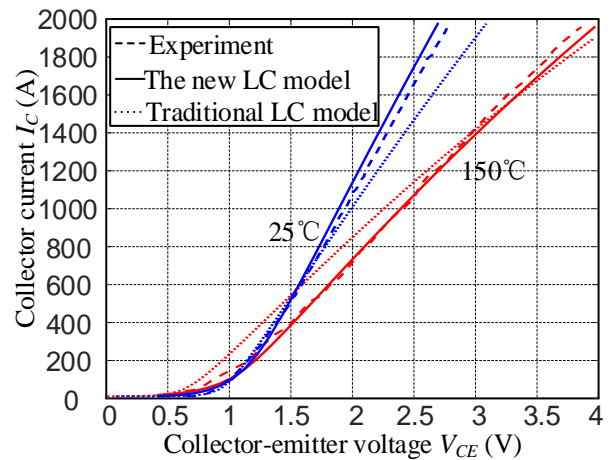


Fig. 7 Comparison of IGBT Static V-I characteristics.

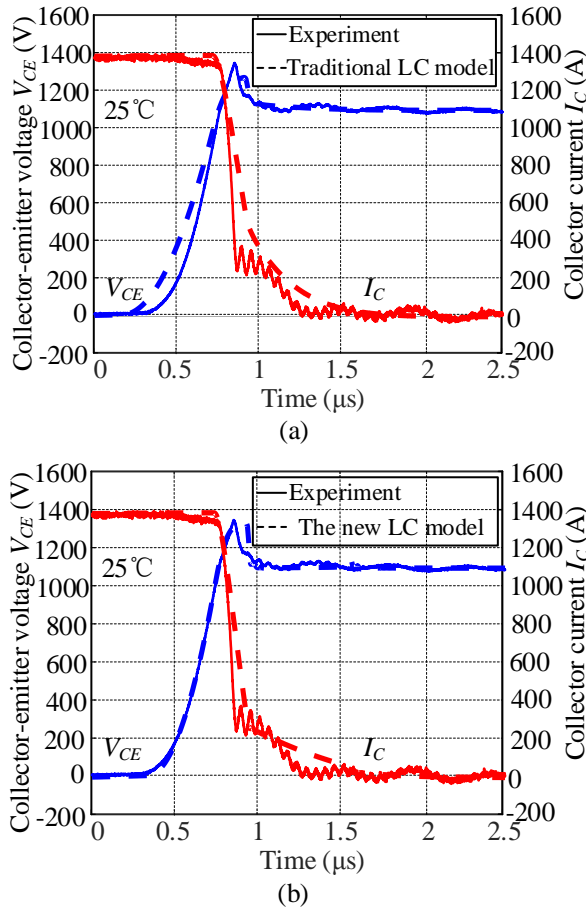


Fig. 8 Turn-off transient characteristics of IGBT at 25°C: (a) The traditional lumped-charge model; (b) The new lumped-charge model.

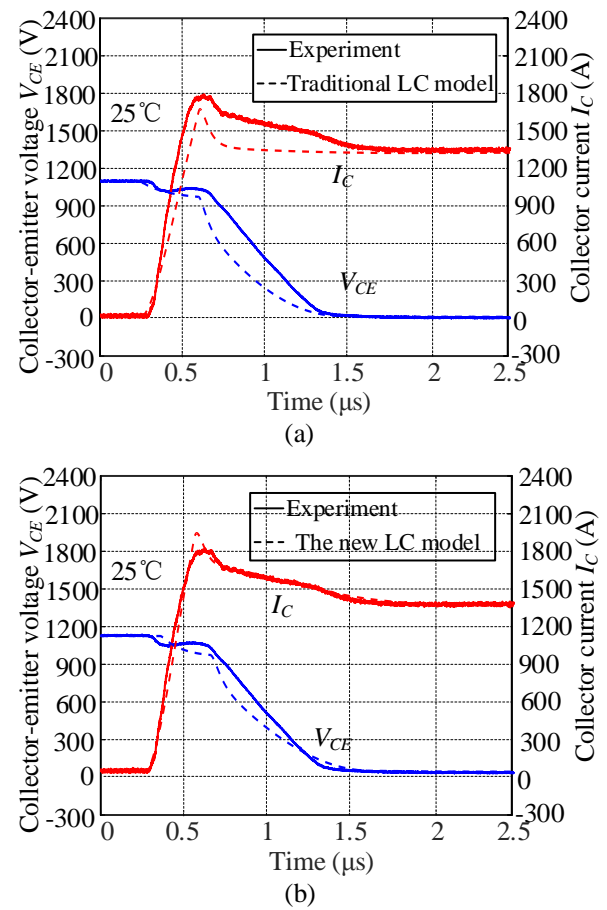


Fig. 9 Turn-on transient characteristics of IGBT at 25°C: (a) The traditional lumped-charge model; (b) The new lumped-charge model.

have high precision at 125°C which is a common working condition for IGBTs. However, the new model could also get higher precision at other temperatures. The switching losses used in this paper is the calculation standard defined by Infineon. The turn-off power losses calculated starting from the moment when the collector voltage rises to 10% of the block voltage, and ending from the moment when the collector current falls to 2% of the conducting current. The turn-on power losses begin at 10% of the collector current and ends at 2% of the block voltage when the collector voltage drops.

#### IV. CONCLUSIONS

A new lumped-charge modeling method is developed for power semiconductor devices in this paper. The new model is proposed to improve the accuracy of the traditional LC model, and verified by an IGBT and PiN diode LC model. From the experiment and simulation results, it can be concluded that: 1) The proposed approach could be used for IGBT modeling. 2) The new model has a higher precision not only in static and transient characteristics, but also in power losses compared to the traditional model. Future research and development on the new method presented in this paper expect to further be applied to other power semiconductor devices including the emerging wide bandgap devices.

TABLE II  
COMPARISON OF TURN-OFF POWER LOSSES

Temp.	Experiment	Traditional LC model (error)	The new LC model (error)
25°C	298.9mJ	522.5mJ (74.8%)	343.7mJ (15.0%)
50°C	331.2mJ	514.1mJ (55.2%)	370.2mJ (11.8%)
75°C	370.1mJ	506.2mJ (36.8%)	413.3mJ (11.7%)
100°C	416.2mJ	498.3mJ (19.7%)	444.9mJ (6.9%)
125°C	467.2mJ	491.0mJ (5.1%)	484.9mJ (3.8%)
150°C	525.5mJ	481.4mJ (-8.4%)	527.6mJ (0.4%)

TABLE III  
COMPARISON OF TURN-ON POWER LOSSES

Temp.	Experiment	Traditional LC model (error)	The new LC model (error)
25°C	961.5 mJ	530.7 mJ (-44.8%)	849.9 mJ (-11.6%)
50°C	1028.3mJ	635.5 mJ (-38.2%)	903.9 mJ (-12.1%)
75°C	1102.2mJ	798.0 mJ (-27.6%)	984.3 mJ (-10.7%)
100°C	1172.6mJ	958.0 mJ (-18.3%)	1080.0mJ (-7.9%)
125°C	1252.9mJ	1042.4mJ (-16.8%)	1184.0mJ (-5.5%)
150°C	1315.8mJ	1057.9mJ (-19.6%)	1244.7mJ (-5.4%)



# ACKNOWLEDGMENT

The authors gratefully acknowledge the financial support from China Scholarship Council (CSC).

# REFERENCES

- [1] S. Kuang, B. W. Williams, and S. J. Finney, "A review of IGBT models," *IEEE Trans. Power Electron.*, vol. 15, no. 6, pp. 1250-1266, Nov. 2000.
- [2] Y. Chen, H. Luo, W. Li, X. He, F. Iannuzzo, and F. Blaabjerg, "Analytical and experimental investigation on a dynamic thermo-sensitive electrical parameter with maximum  $di/dt$  during turn-off for high power trench gate/field-stop IGBT modules," *IEEE Trans. Power Electron.*, vol. 32, no. 8, pp. 6394-6404, Aug. 2017.
- [3] J. Chen, J. Yang, S. Yang, and X. Li, "A coupled circuit-ambipolar diffusion equation model and its solution methodology for insulated gate bipolar transistors," *IEEE Trans. Magnetics*, vol. 53, no. 6, pp. 1-4, 2017.
- [4] P. Xue, G. Fu, and D. Zhang, "Modeling inductive switching characteristics of high-speed buffer layer IGBT," *IEEE Trans. Power Electron.*, vol. 32, no. 4, pp. 3075-3087, 2017.
- [5] M. Riccio, G. D. Falco, P. Mirone, L. Maresca, M. Tedesco, G. Breglio, and A. Irace, "Accurate spice modeling of reverse-conducting IGBTs including self-heating effects," *IEEE Trans. Power Electron.*, vol. 32, no. 4, pp. 3088-3098, 2017.
- [6] S. Ji, T. Lu, Z. Zhao, T. Fujihira, and S. Igarashi, "Physical model with parameter extraction method for Fuji electric 1.7kv IGBT," in *18th Int. Conf. Electrical Machines and Systems* Oct. 2015, pp. 587-590.
- [7] F. Iannuzzo and G. Busatto, "Physical CAD model for high-voltage IGBTs based on lumped-charge approach," *IEEE Trans. Power Electron.*, vol. 19, no. 4, pp. 885-893, Jul. 2004.
- [8] P. O. Lauritzen and C. L. Ma, "A simple diode model with reverse recovery," *IEEE Trans. Power Electron.*, vol. 6, no. 2, pp. 188-191, 1991.
- [9] J. G. Linvill, "Lumped models of transistors and diodes," *Proceedings of the IRE*, vol. 46, no. 6, pp. 1141-1152, 1958.
- [10] C. L. Ma, P. O. Lauritzen, L. Pao-Yi, I. Budihardjo, and J. Sigg, "A systematic approach to modeling of power semiconductor devices based on charge control principles," in *Power Electronics Specialists Conference, PESC '94 Record., 25th Annual IEEE, 20-25 Jun 1994* 1994, pp. 31-37 vol.1.
- [11] C. L. Ma, P. O. Lauritzen, and J. Sigg, "Modeling of power diodes with the lumped-charge modeling technique," *IEEE Trans. Power Electron.*, vol. 12, no. 3, pp. 398-405, May. 1997.
- [12] I. Budihardjo and P. G. Lauritzen, "The lumped-charge power MOSFET model, including parameter extraction," *IEEE Trans. Power Electron.*, vol. 10, no. 3, pp. 379-387, May. 1995.
- [13] C. L. Ma, P. O. Lauritzen, and J. Sigg, "A physics-based gto model for circuit simulation," in *Power Electronics Specialists Conference, 1995. PESC '95 Record., 26th Annual IEEE, vol. 2 18-22 Jun 1995* 1995, pp. 872-878 vol.2.
- [14] F. Iannuzzo and G. Busatto, "A lumped-charge model for gate turn-off thyristors suitable for circuit simulation," *Microelectronics Journal*, vol. 30, no. 6, pp. 543-550, 6/ 1999.
- [15] M. Bellini, I. Stevanovic, and D. Prada, "Improved lumped charge model for high voltage power diode and automated extraction procedure," in *2011 IEEE Bipolar/BiCMOS Circuits and Technology Meeting, 9-11 Oct. 2011* 2011, pp. 49-52.
- [16] P. Leturcq, "Power semiconductor device modelling dedicated to circuit simulation," in *Power Semiconductor Devices and ICs, 1999. ISPSD '99. Proceedings., The 11th International Symposium on, 1999* 1999, pp. 19-26.
- [17] B. J. Baliga, *The IGBT device: Physics, design and applications of the insulated gate bipolar transistor*: William Andrew, 2015.
- [18] [Http://www.Igbtmodel.Org/index.Php?Title=part\\_numbers](http://www.Igbtmodel.Org/index.Php?Title=part_numbers).
- [19] S. Linder, *Power semiconductors*. Italy: EPFL Press, 2006.
- [20] S. Ji, Z. Zhao, T. Lu, L. Yuan, and H. Yu, "HVIGBT physical model analysis during transient," *IEEE Trans. Power Electron.*, vol. 28, no. 5, pp. 2616-2624, May. 2013.
- [21] I. Trintis, T. Poulsen, S. Beczkowski, S. Munk-Nielsen, and B. Rannestad, "Triple pulse tester-efficient power loss characterization of power modules," in *17th European Conference on Power Electronics and Applications*, Sept. 2015, pp. 1-7.
- [22] C. G. Suarez, P. D. Reigosa, F. Iannuzzo, I. Trintis, and F. Blaabjerg, "Parameter extraction for PSpice models by means of an automated optimization tool - an IGBT model study case," in *PCIM Europe 2016; International Exhibition and Conference for Power Electronics, Intelligent Motion, Renewable Energy and Energy Management, 10-12 May 2016*, pp. 1-8.